An Oceano-acoustic Simulation Framework for the Design of Lagrangian Systems Drifting in Mesoscale and Sub-mesoscale Currents

Mathis Grangeon, François-Xavier Socheleau, Aurélien Ponte, Florent Le Courtois, Bazile Kinda

An Oceano-acoustic Simulation Framework for the Design of Lagrangian Systems Drifting in Mesoscale and Sub-mesoscale Currents

Mathis Grangeon*, François-Xavier Socheleau*, Aurélien Ponte†, Florent Le Courtois‡, Bazile Kinda§
*IMT Atlantique, LabSTICC UMR CNRS 6285: {mathis.grangeon,fx.socheleau}@imt-atlantique.fr
†Ifremer: aurelien.ponte@ifremer.fr
†DGA: florent.le-courtois@intradef.gouv.fr
†SHOM: bazile.kinda@shom.fr

***Abstract*—Sub-mesoscale currents are of great interest for oceanographers but unfortunately their observation is a very difficult task. Lagrangian systems can be used to monitor them and require the implementation of an acoustic signal processing chain leading to the localization of each node of that system. In order to help the design of the Lagrangian system prior to sea trials, a simulation framework coupling the results of an oceanographic model with a ray trace software is presented. To illustrate the benefit of this framework, an experimental set-up composed of 5 sources and 20 floats which are drifting for 15 days is analyzed. A dataset of 358,000 frequency responses reflecting sub-mesoscale dynamics is built up. From this dataset, relevant statistics are calculated to define the best transmission parameters of the acoustic sources and to choose the right ranging method. It turns out that using pseudo-random sequences and allocating the spectral resources with Code Division Multiple Access method is a relevant design in our context. Also, it appears that a non-coherent ranging processor gives the best performance.**

***Index Terms*—Lagrangian systems, underwater acoustics, localization, signal detection, spectrum sharing.**

I. Introduction

The upper layers of the ocean are a focal point for oceanographers due to the complex physical dynamics that occur there, including sub-mesoscale processes and internal waves. Such features have a temporal scale varying between 1 hour and several days. Their spatial scale are less than 10 kilometers. These phenomena are particularly intense in tumultuous oceanic regions. and are closely linked to the transport of organic carbon and plankton. As our understanding of these dynamics grows, so does our knowledge of the underwater ecosystem. While several ocean circulation models exist, observing these movements remains a challenge. Fortunately, literature suggests that Lagrangian systems are well-suited to overcome these hurdles [1]. By monitoring a swarm of sensors drifting within sub-mesoscale currents, we can create a detailed 3D reconstruction of the currents of interest. Figure 1 shows an experimental Lagrangian system with subsurface acoustic sources localized and synchronized by GPS. After transmission, their signals are detected by passive floats equipped with hydrophones, and these floats are then geolocalized by triangulation.

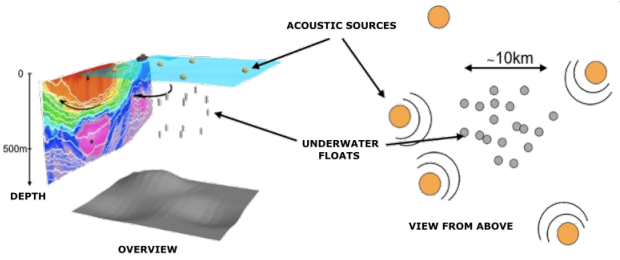

Fig. 1: Scheme of a Lagrangian system

However, implementing this technique requires careful consideration of design parameters. Seawater is highly absorbent of electromagnetic waves, which means that acoustic signals are the best option for transmitting information between sources and floats. Due to relative motion between sources and receivers, acoustic signals are impacted by Doppler effects. This is accompanied by a multi-path effect due to the variability of sound speed and the interactions with the surface and/or the bottom, making the underwater acoustic channel (UAC) multi-scale multi-lag (MSML) [2]. On the top of that, these channel characteristics strongly depend on the period of time and the zone where the system is deployed. The same applies for the type of noise encountered and the available bandwidth. This means that the signals and the processing must be adapted to the drifting area in order to increase the accuracy of the observations. In addition, signals transmitted by different subsurface acoustic sources must not collide to achieve good performance. The scheduling and spectrum sharing methods must therefore be carefully designed.

To derive guidelines for the design of Lagrangian systems, we built a realistic framework by coupling together oceanographic and acoustic simulations. More precisely, we derived transducers trajectories and sound speed field from a *Coastal and Regional Ocean COmmunity model* (CROCO) [3]. These are the inputs of a ray propagation model (Bellhop) [4] which provides all needed variables to construct the channel time-varying responses (TVR). In this way, each TVR takes into account both spatial and temporal variability of the medium. The objective of this paper is to promote the use of such a simulator for the the design of Lagrangian systems. To do so, we conduct a statistical analysis of the oceano-acoustic

simulator output to extract guidelines for the choice of (i) the signal to be transmitted, (ii) the spectrum sharing method between sound sources and (iii) the detection and ranging algorithm at reception. A specific scenario corresponding to the dynamics encountered during autumn 2010 in the Gulf of Biscay is studied.

The paper is organized as follows. Section II describes the simulator as well as the environment considered to design the Lagrangian system. Section III introduces the signal processing chain to locate the drifters and discuss the possible design options. Section IV presents the results from which design guidelines are derived. Section VI concludes by summarizing our work and outlines the main remarks.

II. The oceano-acoustic simulator

A. The need of a realistic environment

As mentioned in the introduction, our Lagrangian system is supposed to drift within sub-mesoscale features, which have specific dynamics such as currents or temperature variations for example. Those particular dynamics have a strong impact on the way acoustic signals propagate within their environment. In this section, we give more details about how we inject sub-mesoscale dynamics into acoustic propagation model in order to get a realistic dataset.

B. An oceano-acoustic dataset

The foundation of our numerical modeling of signal propagation in UAC from sub-mesoscale structures is the results of the CROCO model, with the configuration BOB1000 that is the evolution of three-dimensional currents and tracers (temperature, salinity) within the Gulf of Biscay [3]. The numerical simulation grid has 40 stretched vertical levels and an approximate horizontal spacing of 1km (curvilinear horizontal grid). Forcings include tides (FES2014 [5]), atmospheric forcing (ALADIN MeteoFrance [6]) and river discharges.

Figure 2 shows a snapshot of this oceanographic simulation where 5 sources and 20 floats are drifting with the currents derived from [3]. Float and source trajectories are performed offline with the OceanParcels library [7] and hourly model outputs fields. The drifter simulations are performed over a time period of 15 days (2010/09/01 to 2010/09/15) and predict the evolution of platforms released around an offshore location (45N, 6W). All these propagation environments constitute a large number of inputs for a numerical acoustic propagation model, such as *bellhop* [4]. Using this software across all oceanographic results completes our oceanographic dataset from an acoustic point of view, providing signal arrival times via the ray tracing method [8], [9]. The amplitudes of the paths are also calculated, and knowledge of the position of the floats and sources over time also gives us access to their relative velocities and hence Doppler compression factor. For each source-receiver pair over the 15 days of drift, a total of 358,000 channel responses are modeled. The depth of the sources is fixed to 5 m and the floats are drifting at 200 m of depth. This placement corresponds to a sea trial where the floats are in a zone of interest and each source is suspended from a buoy by a cable. The frequency used for the ray traces

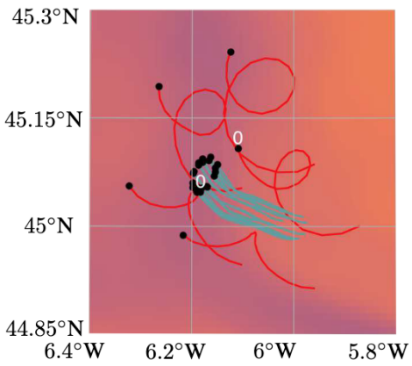

Fig. 2: Deployment example of an experimental system (sources in red, floats in blue) on a temperature cartography (18°C in blue, 20°C in orange)

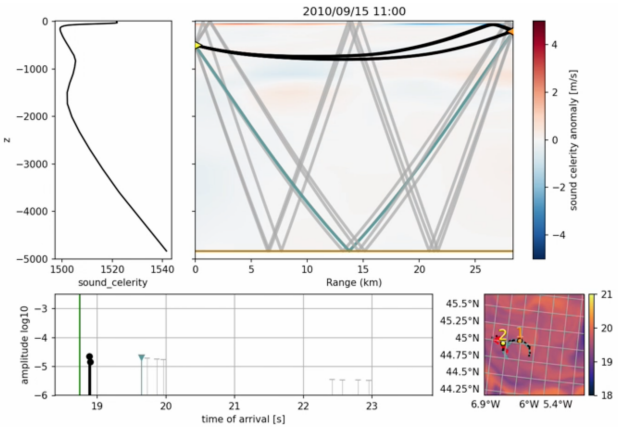

Fig. 3: Example of an oceano-acoustic simulation snapshot

computation is 3750 Hz and we consider a 2.5 kHz bandwidth. These spectrum settings were chosen in view of the targeted propagation distances and the technology we could deploy.

III. Signal processing chain and design options

A. Problem formulation

Float localization is made possible by converting a set of acoustic time series into georeferenced coordinates using time-of-arrival (ToA) measurements. This conversion is usually performed in four steps:

1) Each signal transmitted by the subsurface sources is detected.
2) Form the detected signal, the channel parameters are estimated (time-of-arrival, amplitude etc.).
3) By matching the estimated channel parameters with those obtained with an acoustic propagation model, the range between the source and the float are estimated.
4) Based on the set of estimated ranges, each float is then localized by triangulation [10], [11].

In the sequel, we briefly review each step and discuss the possible design options.

B. Signal detection and channel estimation

For a given float, the baseband signal $y_n(t)$ observed at reception is either modeled as

$$\mathcal{H}_0 : y_n(t) = w(t), \tag{1}$$

when no signal is transmitted or as

$$\mathcal{H}_1 : y_n(t) = \sum_{l=0}^{L_n-1} \alpha_{n,l} s_n(t - \tau_{n,l}(t)) e^{-i2\pi f_c \tau_{n,l}(t)} + w(t), \tag{2}$$

when $s_n(t)$ is the signal transmitted by the n^{th} source. $\alpha_{n,l}(t)$ denotes the complex attenuation of the l-th channel tap, f_c is the carrier frequency and $\tau_{n,l}(t)$ is the delay assumed to be a linear function of time described by an initial delay $\tau^0_{n,l}$ and a drift $\epsilon_{n,l}$ (also called the Doppler scale or the time-compression factor), so that $\tau_{n,l}(t) = \tau^0_{n,l} + \epsilon_{n,l} t$. $w(t)$ is the additive noise. The UAC associated with this type of observation is known as multi-scale multi-lag (MSML) [2], [12]. The MSML model is quite comprehensive in terms of the phenomena it models [13]. It reflects the multipath, Doppler scaling and attenuation phenomena experienced by signals as they propagate. Based on (2), the frequency response of the channel can be expressed as

$$h_n(f,t) = \sum_{l=0}^{L_n-1} \alpha_{n,l} e^{-i2\pi(f+f_c)(\tau^0_{n,l}+\epsilon_{n,l}t)}. \tag{3}$$

Based on the observation $y_n(t)$ and the knowledge of $s_n(t)$, the problem is first to decide between the two hypotheses $\mathcal{H}_0$ and $\mathcal{H}_1$, and then, when $\mathcal{H}_1$ is decided, to estimate the unknown channel parameters $\left\{ L_n, \left(\alpha_{n,l}, \tau^0_{n,l}, \epsilon_{n,l} \right)_{\{l=0,\cdots,L-1\}} \right\}$.

The literature proposes several methods for detecting signals of interest and jointly estimating the parameters of the UAC model (3). For example, in [14]–[16] the estimation is performed with a *matching-pursuit* algorithm, taking advantage of the fact that the UAC defined in (3) is sparse. Observations are projected onto a set of compressed and delayed replicas of the source signal (i.e. a signal subspace). In an iterative manner, atoms in the subspace are removed from the observation, so that the energy within the observation is reduced if signals of interest are present. Detection generally works if some prior knowledge about the channel, such as the signal-to-noise ratio or the degree of sparsity is accessible. To overcome this limitation, the author in [2] proposes to combine a matching-pursuit algorithm with a generalized likelihood framework [17]. Although these methods can be used to estimate the channel frequency responses, their computational complexity makes them difficult to be used on a large dataset such as the one presented in Sec. II. A less complex approach is the traditional bank of matched filters (BMF) with Doppler replicas [18] that can be implemented with FFT-based filtering. As shown in Sec. IV, it provides satisfying results in our context. Choices must then be made on the following parameters to maximize the detection and estimation performance:

- The signal $s_n(t)$ to transmit.

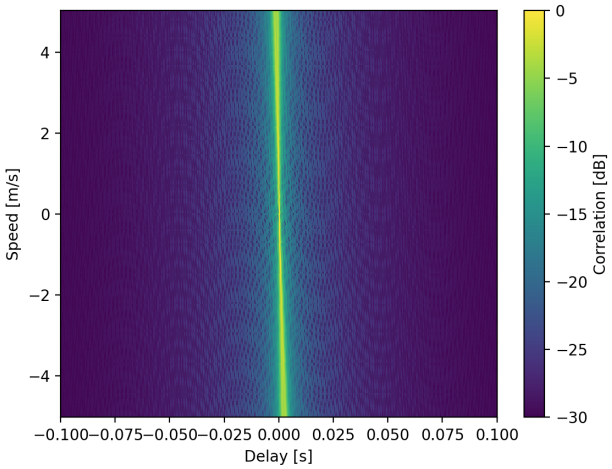

Fig. 4: Chirp Ambiguity function

- The spectrum sharing method to avoid collision between signals.
- Range and resolution of the relative velocity that must be captured by the bank of matched filters.

Unlike the first two parameters, the design of the BMF does not call for specific arbitrage between several solutions. As discussed in Sec. IV, the design will simply be chosen based on the output of the simulator.

1) Signal to transmit: To get accurate estimates of the channel parameters, the transmitted signal must have good correlation properties in MSML environments. These properties are fully described by the ambiguity function of transmitted signal $s_n(t)$. Although, it exists a wide range of choices to design our emission process, we here focus on chirps and pseudo-random binary sequences, which are often used in sonar applications [13], [19]. More specifically, we consider a linear chirp and a Gold sequence of duration 0.5 s. The Gold sequence is made of 1023 bits with a symbol rate of $\approx$ 2272 Bd and a root raised cosine filter with roll-off set to 0.1. Fig. 4 and 5 show the ambiguity functions of the selected signals. Despite the strong correlation peak, one can also observe in Fig. 4 that there is a coupling between the delay and the Doppler compression. Thus, the chirp can be easily detected but the estimation of its arrival time may be biased in case of motion. On the other hand, the Gold sequence does not exhibit coupling but its correlation peak is embedded in a correlation clutter, making its detection more delicate. In addition to their different properties, Gold sequences allow sources to be differentiated by code division multiple access, which is not the case with linear chirps. Nonlinear chirps are required to use this method of spectral resource allocation, which can complicate the coupling between delays and Doppler compression.d

Sec. IV presents some results obtained with our oceano-acoustic framework that are helpful in choosing between the two options.

2) Spectrum sharing: As shown in Fig. 1, multiple sources emits. This means that limited spectral resources must be shared. In the underwater acoustic community, the channel multiple access problem has usually been addressed in the

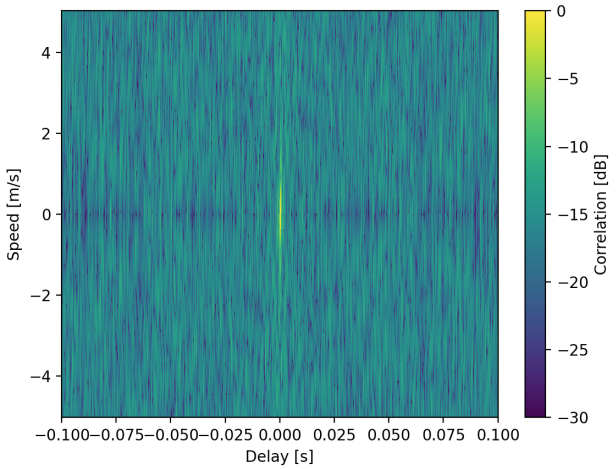

Fig. 5: Gold sequence ambiguity function

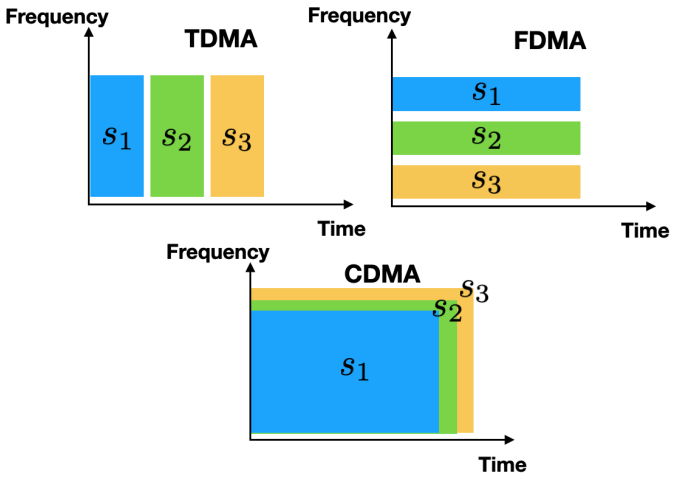

Fig. 6: Scheme of the method of spectrum resource sharing

context of communication and networking. In this context, spectrum sharing methods have been improved especially in terms of bit rate [20], [21]. However, in our application, acoustic signals are the vectors for inferring position of the floats and not to communicate in the strict sense. In this context the multiple access method used in underwater acoustics are [22]:

- Time Division Multiple Access (TDMA)
- Frequency Division Multiple Access (FDMA)
- Code Division Multiple Access (CDMA)

This three techniques are illustrated in Figure 6. The main objective of these techniques is to provide orthogonality between sources in order to differentiate them within the time series sensed by the floats. The TDMA method does this by allocating a period of emission to each sources. In our system only the sources are synchronized via GPS. Also, since the float position is unknown a priori, there is not guarantee that the orthogonality will be maintained at reception due to unknown varying propagation delays. This prevent us from using this method. With FDMA, the orthogonality is achieved by allocating a different sub-band to each source. This method provides a perfect orthogonality but the sources having the higher sub-bands are disadvantaged since the absorption is more preponderant. Reducing the bandwidth also leads to worse temporal resolution for ToA estimation. In contrast, with CDMA all the sources use the total bandwidth so the temporal resolution is better. In addition, CDMA exploits the full frequency diversity offered by the channel as opposed to FDMA. However, there is only a pseudo-orthogonality between the sources. This results in potential inter-source interference and near-far problems [23]. Again, to choose the suitable method, our oceano-acoustic dataset can provide useful information. For instance, results on the probability of collision between sources and on the robustness to the near-far effect are analyzed in Sec. IV.

C. Ranging

Ranging is commonly solved as an inverse problem [24]–[27]. Based on the estimates $\left\{\hat{L}_n, (\hat{\alpha}_{n,l}, \hat{\tau}^0_{n,l}, \hat{\epsilon}_{n,l})_{l=0,..,\hat{L}_n-1}\right\}$, the estimated channel frequency response at the time of transmission can be derived and discretized in frequency to produce the vector $\hat{\boldsymbol{h}}_n = [\hat{h}_n(f_0), \cdots, \hat{h}_n(f_{K-1})]^T$, where

$$\hat{h}_n(f_k) = \sum_{l=0}^{\hat{L}_n-1} \hat{\alpha}_{n,l} e^{-i2\pi(f_k+f_c)\hat{\tau}^0_{n,l}}. \tag{4}$$

By comparing $\hat{\boldsymbol{h}}_n$ with the output of a channel simulator, the range and the depth of the float can be inferred, provided that the acoustic environment is well known. More specifically, an underwater acoustic propagation model, like *Bellhop* [4], is used to compute replicas of (3), denoted $\boldsymbol{g}(\boldsymbol{\theta})$ for several candidate positions $\boldsymbol{\theta} = [r, d]$, where r denotes range under test between the source and the float and d is the candidate depth of the float. As depicted in Fig. 7, the matching between the observation $\hat{\boldsymbol{h}}_n$ and its replicas is made with a *processor* also called *cost function*, denoted $c(\boldsymbol{g}(\boldsymbol{\theta}), \hat{\boldsymbol{h}}_n)$. By applying it for several candidates, our replicas grid is turned into an ambiguity grid which quantifies the match between the observed frequency response and its replicas. The range and depth position from the n-th source is then obtained by solving

$$\hat{\boldsymbol{\theta}}_n = \underset{\boldsymbol{\theta}}{\operatorname{argmax}}\ c(\boldsymbol{g}(\boldsymbol{\theta}), \hat{\boldsymbol{h}}_n). \tag{5}$$

The main design choice for ranging is then the cost function c. Two options are considered. A coherent processor that keeps the phase information of the channel and a non-coherent processor that removes the phase information from the comparison. They can be expressed, respectively, as [27]

$$c_{coh}(\boldsymbol{g}(\boldsymbol{\theta}), \hat{\boldsymbol{h}}_n) = \frac{|\boldsymbol{g}(\boldsymbol{\theta})^H \hat{\boldsymbol{h}}_n|^2}{\|\boldsymbol{g}(\boldsymbol{\theta})\|_2^2 \|\hat{\boldsymbol{h}}_n\|_2^2} \tag{6}$$

and

$$c_{ncoh}(\boldsymbol{g}(\boldsymbol{\theta}), \hat{\boldsymbol{h}}_n) = \frac{|\tilde{\boldsymbol{g}}(\boldsymbol{\theta})^H \hat{\tilde{\boldsymbol{h}}}_n|^2}{\|\tilde{\boldsymbol{g}}(\boldsymbol{\theta})\|_2^2 \|\hat{\tilde{\boldsymbol{h}}}_n\|_2^2} \tag{7}$$

where

$$\hat{\tilde{\boldsymbol{h}}}_n = \mathcal{F}\{|\mathcal{F}^{-1}\{\hat{\boldsymbol{h}}_n\}|\}, \tag{8}$$

and

$$\tilde{\boldsymbol{g}}(\boldsymbol{\theta}) = \mathcal{F}\{|\mathcal{F}^{-1}\{\boldsymbol{g}(\boldsymbol{\theta})\}|\}. \tag{9}$$

$\mathcal{F}$ and $\mathcal{F}^{-1}$ denote the discrete Fourier transform and inverse discrete Fourier transform, respectively.

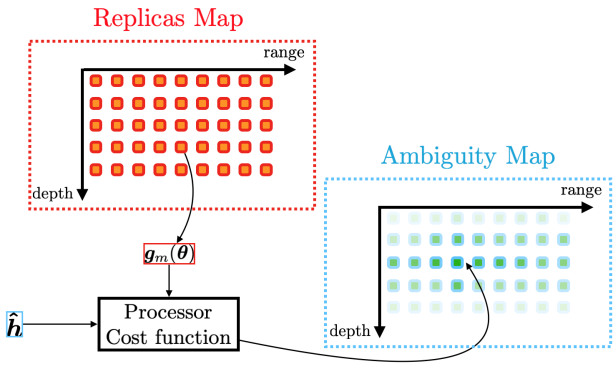

Fig. 7: Overview of the ranging method

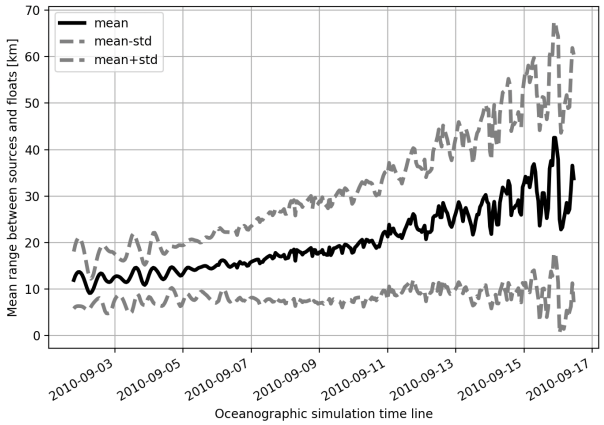

Fig. 8: Mean distance between sources and floats as a function of time

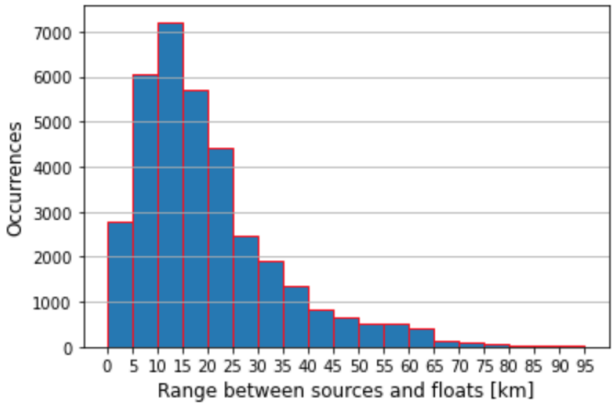

Fig. 9: Distribution of the ranges between sources and floats

D. Localization

Estimating the distance from a source to a single float is not sufficient to accurately determine the position of that float. In underwater acoustic (UWA), localization is usually achieved by trilateration. More specifically, the float's coordinates are computed by solving an inverse problem over the estimated distances and several candidate positions. Often the problem solved is range-least square (R-LS), but other least square methods can also be used [10], [11]. Despite the obvious link between ranging performance and the localization method, there is very little choice in this part of the processing chain in terms of design, other than the number of sources that can affect localization accuracy. Moreover, since localization by solving R-LS problems provides quite good accuracy for a reasonable computational cost, it is very suitable for our framework.

IV. Design Guidelines

The purpose here is to optimize the monitoring of our Lagrangian system by determining the design of our signal processing chain. In this section, all the points mentioned above (transmitted signal, spectrum sharing...) are discussed using appropriate quantities. This is an example of how coupling oceanographic results with an acoustic propagation model can be a powerful tool for conceptualizing ocean exploration systems. The same approach can be used to focus the analysis on other aspects and to derive other useful guidelines for the design of other underwater acoustic systems.

A. Statistics on the oceano-acoustic simulation

In this subsection, we focus on the overall statistics about the underwater environment to properly design the transmitted signals and the spectrum sharing method as well as to tune the BMF at reception. Fig. 8 shows the average distance between the sources and the floats at every time steps of the oceano-acoustic simulation. We can see that the average distance tends to increase slowly. The mean distance ranges from a dozen kilometers to twice that in 10 days. It is only after this period that the floats really spread out relative to the sources. This slow dispersion is also reflected in Fig. 9 that shows the distribution of relative distances. We can see that the majority of distances are around 15 km.

Also, Fig 10 shows that the majority of relative velocities between sources and floats are between -0.5 and 0.5 m/s, which also explains the slow dispersion of the system. These observations indicate that the system that tends to remain grouped despite several days of drift. This may cause inter-source interference. In this case, the CDMA method may be more complicated to use than the FDMA method, since the last one provides a strict orthogonality between every sources.

Moreover, with the ToA and distance cross-distribution shown in Fig. 11, we observe that, for the most common distances, the ToAs are distributed around three clusters located at 10, 15 and 20 seconds, respectively. This means that UWA channels are likely to be frequency selective, due to the multipath effects. This is an indication in favor of CDMA-type spectrum sharing. This contradicts the previous suggestion. Figures 8-11 are therefore not sufficient to define an adequate transmission strategy for tracking the float pack. Nevertheless, they illustrate the overall behavior of the system, highlighting frequently encountered UWA channels. Finally, Fig. 11 shows that almost all propagation times are less than a minute, which is an indication of the periodicity of signal transmission for

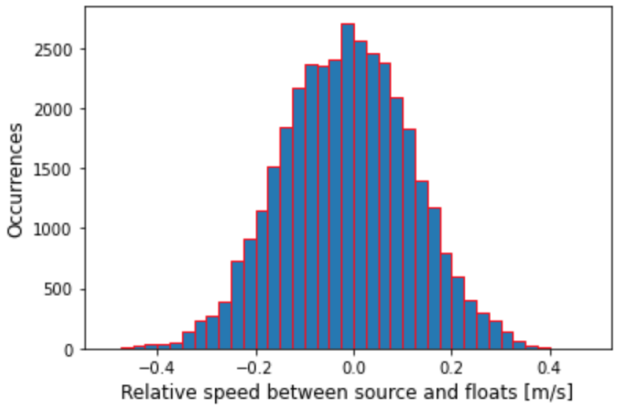

Fig. 10: Distribution of the relative velocities between sources and floats

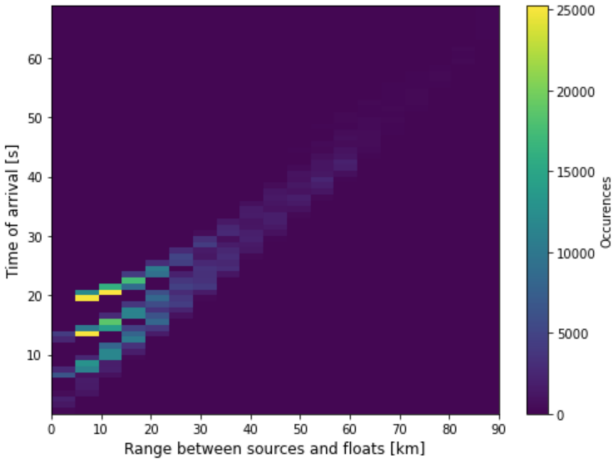

Fig. 11: ToA distribution as a function of distance

tracking the floats. Figure 10 shows that the relative velocities are all between -0.5 and 0.5 m/s, allowing us to tune the Doppler replicas of the BMF.

B. Choice of the emitted signal

To deepen the design of our Lagrangian system in terms of transmitted signal, we present the robustness of the cost function (6) and (7) to noise and inter-source interference. The following results have been obtained at the float positions returned by our simulation, with the signals presented in Sec. III-B. More precisely, these transmitted signals are filtered with the 358,000 channel responses of the oceano-acoustic providing 358,000 signals at reception. Then, either noise or interference is added to the signals at reception. After the signal detection and the channel estimation is done, the coherent and incoherent cost functions are computed. In this way, the performance of our processors all over the oceano-acoustic simulation is obtained. Fig. 12 shows the average performance over the whole simulation as a function of SNR for both the chirp and the Gold sequence. The values of the processors are computed at the right location. It shows that the coherent processor (6) gives the poorest performance, indicating that the phase of the received signals is difficult

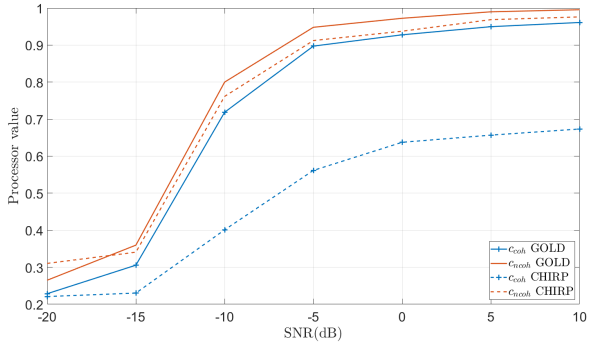

Fig. 12: Average processors performance as a function of SNR

to estimate. This is particularly true for the chirp since its ambiguity function 4 shows that ToA estimation depends on the Doppler scale factor. This suggests a preference for the non-coherent processor for ranging. We also observe that Gold sequence provides the best correlation between simulation results and our observations with the BMF. In light of these observations, our performance study is then conducted by only considering the case of the non-coherent processor employed with the Gold sequence.

C. Choice of the spectrum sharing method

As discussed in Sec. III-B2, to fully define the emission part of our Lagrangian system, we must decide between FDMA and CDMA to share the spectral resources between our several sources. To do so, the resistance of CDMA to the near-far effect dur to inter-source interference as well as a probability of signal collision must is analyzed next.

Fig. 13 represents the average performance of processor (7) with the Gold sequence as a function of the signal-to-interference ratio (SIR) defined as

$$SIR = 10\log_{10}\left(\frac{\int_{\mathbb{R}} |x_n(t)|^2\, dt}{\sum\limits_{m\neq n}\int_{\mathcal{I}_n} |x_m(t)|^2\, dt}\right) \qquad (10)$$

where $x_n(t)$ denotes the received signal without noise, i.e. $x_n(t) = y_n(t) - w(t)$ and $\mathcal{I}_n = \text{supp}\,(x_n(t))$ is the support of $x_n(t)$.

These results are obtained with a SNR of -5 dB. For this pessimistic scenario, we observe that the inter-source interference phenomenon significantly deteriorates the channel estimation as soon as the SIR is lower than -8 dB. In other words, as long as the power of the interference is less than six times than the power of the signal of interest, the performance is not significantly affected.

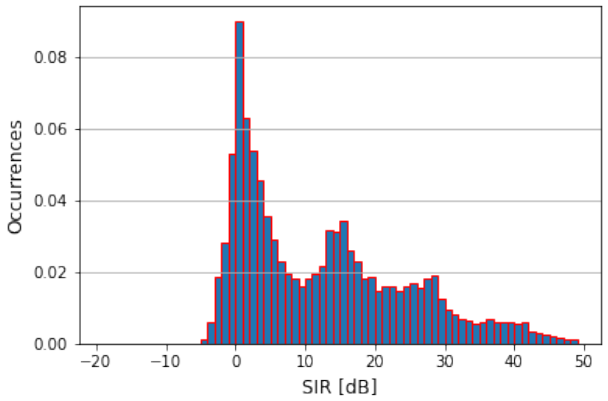

Fig. 14: Distribution of the SIR

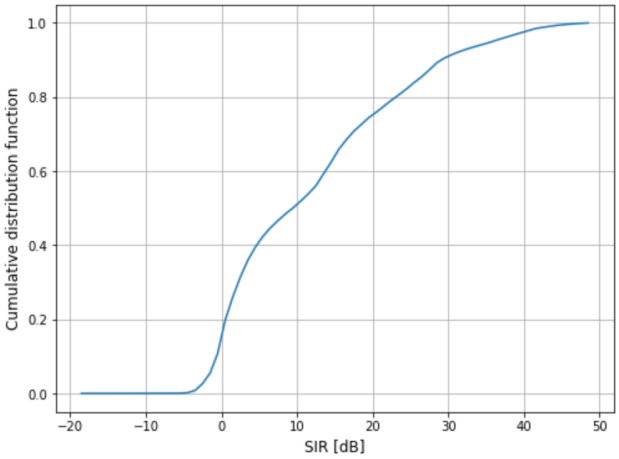

Fig. 15: Cumulative distribution function of the SIR

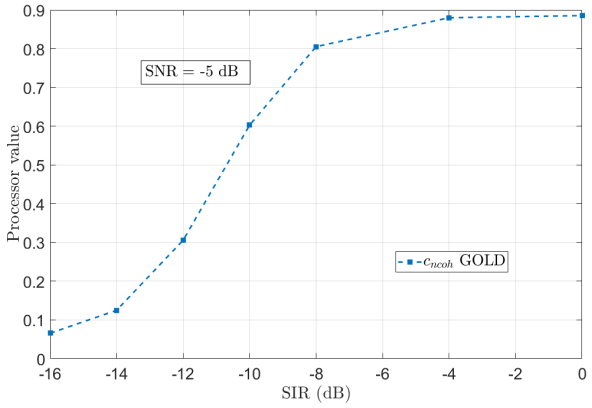

Fig. 13: Non-coherent processor as a function of signal-to-interference ratio

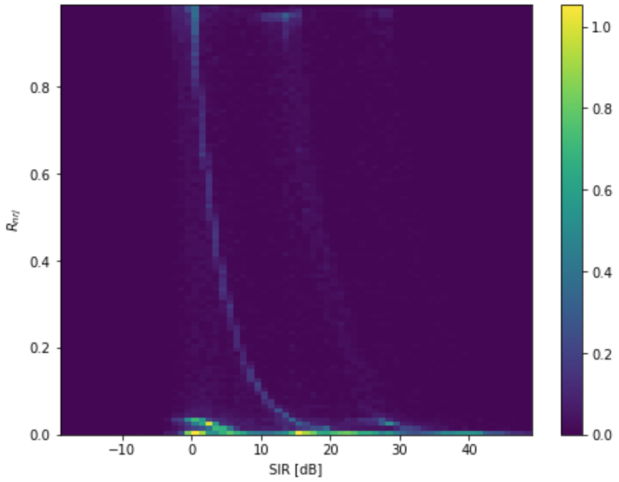

Fig. 16: R_{nrj} and SIR cross-distribution

Figure 14 presents the SIR distribution all over the oceano-acoustic simulation. It shows that almost all SIR are greater than -8 dB. This is emphasized by Fig. 15, which shows that the probability of having a SIR below 0 dB is almost zero. These results suggest that the inter-source interference phenomenon is not strong enough to degrade the channel estimation process and our ranging method.

To further analyze the effect of interference due to collisions, we also measure the proportion of the signal of interest that is affected by interference. This is measured by the following metric

$$R_{nrj} = \frac{\int_{\mathbf{J}_n} |x_n(t)|^2 \, dt}{\int_{\mathbb{R}} |x_n(t)|^2 \, dt} \tag{11}$$

where $\mathbf{J}_n = \bigcup_{m \neq n} (\text{supp}(x_m) \cap \text{supp}(x_n))$.

The distribution of R_{nrj} as a function of the SIR is shown in Fig. 16. As expected, the greater the overlap between signals the lower the SIR. However, the most common behavior is that the SIR is around 0 despite a few amount of interfered energy. This is explained by the fact that when signals from different sources collide, only the secondary paths are affected by the main paths of the interfering source.

In summary, the inter-source interference phenomenon mainly concerns the secondary paths, which are also the most difficult to detect. From this point of view, inter-source interference is really not predominant in our simulation. That is why it is preferable to use CDMA-type spectrum sharing.

V. Conclusion

To design a Lagrangian system for exploring mesoscale and sub-mesoscale ocean structures, we have introduced a simulation framework coupling oceanographic results with an acoustic propagation model. This framework is intended to be as representative as possible of the true environment in which the system evolves. To demonstrate the usefulness of this simulation, we have detailed the signal processing chain leading to the localization of the float swarm and proposed different options to optimize it. Simulations show that using Gold sequences with a CDMA type of spectrum sharing proves to be a relevant transmission choice for our localization process. By using the whole band, the transmission process is more resistant to frequency selectivity and the temporal resolution of the ToA estimation is also improved. Despite the risk of collision between signals, transmission is resistant

to interference down to an SIR level of -8 dB. Also, it appears that secondary paths of the frequency responses are the more impacted by collisions.

In this paper, we have shown how the coupling of acoustic and oceanographic knowledge can be an interesting tool in the design of marine applications. For future work, we plan to study the float localization error with our simulation framework and incorporate uncertainties. Depending on these future results, sea trials may be conducted.

VI. Acknowledgments

This work was funded by the French Defense Innovation Agency (AID) and the Brittany region.

References

[1] Jules S Jaffe, Peter JS Franks, Paul LD Roberts, Diba Mirza, Curt Schurgers, Ryan Kastner, and Adrien Boch, "A swarm of autonomous miniature underwater robot drifters for exploring submesoscale ocean dynamics," Nature communications, vol. 8, no. 1, pp. 14189, 2017.

[2] François-Xavier Socheleau, "Joint signal detection and channel estimation in multi-scale multi-lag underwater acoustic environments," in Proceedings of Meetings on Acoustics UACE. Acoustical Society of America, 2021, vol. 44, p. 055001.

[3] Sebastien Theetten and Guillaume Charria, "Description de la configuration régionale bob400 du modèle croco (bay of biscay 400 mètres de résolution spatiale horizontale)," 2020, DOI: 10.13155/74855.

[4] Michael B Porter, "The bellhop manual and user's guide: Preliminary draft," Heat, Light, and Sound Research, Inc., La Jolla, CA, USA, Tech. Rep, vol. 260, 2011.

[5] Florent H Lyard, Damien J Allain, Mathilde Cancet, Loren Carrère, and Nicolas Picot, "Fes2014 global ocean tide atlas: design and performance," Ocean Science, vol. 17, no. 3, pp. 615–649, 2021.

[6] P Daniel, P Josse, and V Ulvoas, "Atmospheric forcing impact study in meteo-france storm surge mode," WIT Transactions on The Built Environment, vol. 58, 2001.

[7] Philippe Delandmeter and Erik Van Sebille, "The parcels v2. 0 lagrangian framework: new field interpolation schemes," Geoscientific Model Development, vol. 12, no. 8, pp. 3571–3584, 2019.

[8] Rodney FW Coates and RFW Coates, Underwater acoustic systems, Springer, 1990.

[9] Manfred Kaltenbacher, Computational acoustics, Springer, 2018.

[10] Amir Beck, Petre Stoica, and Jian Li, "Exact and approximate solutions of source localization problems," IEEE Transactions on signal processing, vol. 56, no. 5, pp. 1770–1778, 2008.

[11] Darya Ismailova, Localization algorithms for passive sensor networks, Ph.D. thesis, 2016.

[12] Paul A Van Walree and Roald Otnes, "Ultrawideband underwater acoustic communication channels," IEEE Journal of Oceanic Engineering, vol. 38, no. 4, pp. 678–688, 2013.

[13] Paul van Walree, "Channel sounding for acoustic communications: techniques and shallow-water examples," 2011.

[14] Weichang Li and James C Preisig, "Estimation of rapidly time-varying sparse channels," IEEE Journal of Oceanic Engineering, vol. 32, no. 4, pp. 927–939, 2007.

[15] Yi Zhang, Ramachandran Venkatesan, Octavia A Dobre, and Cheng Li, "Efficient estimation and prediction for sparse time-varying underwater acoustic channels," IEEE Journal of Oceanic Engineering, vol. 45, no. 3, pp. 1112–1125, 2019.

[16] Xue Jiang, Wen-Jun Zeng, and Xi-Lin Li, "Time delay and doppler estimation for wideband acoustic signals in multipath environments," The Journal of the Acoustical Society of America, vol. 130, no. 2, pp. 850–857, 2011.

[17] Francois-Xavier Socheleau, "A multifamily glrt for cfar detection of signals in a union of subspaces," IEEE Signal Processing Letters, vol. 27, pp. 2104–2108, 2020.

[18] Paul A van Walree, François-Xavier Socheleau, Roald Otnes, and Trond Jenserud, "The watermark benchmark for underwater acoustic modulation schemes," IEEE journal of oceanic engineering, vol. 42, no. 4, pp. 1007–1018, 2017.

[19] Nadav Levanon, "Radar principles," New York, 1988.

[20] M Stojanovic, L Freitag, and M Johnson, "Channel-estimation-based adaptive equalization of underwater acoustic signals," in Oceans' 99. MTS/IEEE. Riding the Crest into the 21st Century. Conference and Exhibition. Conference Proceedings (IEEE Cat. No. 99CH37008). IEEE, 1999, vol. 2, pp. 985–990.

[21] Ahmad RS Bahai, Burton R Saltzberg, and Mustafa Ergen, Multi-carrier digital communications: theory and applications of OFDM, Springer Science & Business Media, 2004.

[22] Ethem M Sozer, Milica Stojanovic, and John G Proakis, "Underwater acoustic networks," IEEE journal of oceanic engineering, vol. 25, no. 1, pp. 72–83, 2000.

[23] DAVID J Goodman and Adel AM Saleh, "The near/far effect in local aloha radio communications," IEEE Transactions on vehicular technology, vol. 36, no. 1, pp. 19–27, 1987.

[24] Stan E Dosso and Michael J Wilmut, "Maximum-likelihood and other processors for incoherent and coherent matched-field localization," The Journal of the Acoustical Society of America, vol. 132, no. 4, pp. 2273–2285, 2012.

[25] Yann Le Gall, Stan E Dosso, François-Xavier Socheleau, and Julien Bonnel, "Bayesian source localization with uncertain green's function in an uncertain shallow water ocean," The Journal of the Acoustical Society of America, vol. 139, no. 3, pp. 993–1004, 2016.

[26] Yann Le Gall, Francois-Xavier Socheleau, and Julien Bonnel, "Matched-field processing performance under the stochastic and deterministic signal models," IEEE Transactions on Signal Processing, vol. 62, no. 22, pp. 5825–5838, 2014.

[27] Pan He, Lu Shen, Benjamin Henson, and Yuriy V Zakharov, "Coarse-to-fine localization of underwater acoustic communication receivers," Sensors, vol. 22, no. 18, pp. 6968, 2022.